ALICE/SIL 98-05
Internal Note-SIL
22 January 1998

IN-BEAM TEST OF DOUBLE-SIDED SILICON STRIP DETECTOR

L. Arnold, J. Baudot, J.P. Coffin, G. Guillaume, S. Higueret, P. Fintz, F. Jundt, C. Kuhn, J.R. Lutz, P. Pagès, S. Pozdniakov, F. Rami

Institut de Recherches Subatomiques (IReS), IN2P3-CNRS/ULP
23, rue du Loess, 67037 Strasbourg CEDEX 2, France

S. Bouvier, B. Erazmus, S. Giliberto, L. Martin, C. Le Moal, C. Roy

SUBATECH, Université de Nantes/Ecole des Mines de Nantes/IN2P3/CNRS
44070 Nantes, France

C. Colledani, W. Dulinski, R. Turchetta

Laboratoire d'Electronique et de Physique des Systèmes Instrumentaux (LEPSI)
23, rue du Loess, 67037 Strasbourg CEDEX 2, France

Abstract

The response of a double-sided silicon strip detector to a 3 GeV pion beam from the Proton Synchrotron at CERN is presented. Charge matching between the pulseheights from both sides, produced by the same traversing particle, is obtained with a resolution better than 5%. The spatial resolution is measured as a function of the incident angle of the projectile, varying from 15μm at normal incidence to 32μm at 45^o. The contribution of multiple scattering to the spatial resolution is estimated to 11μm.

1 Introduction

Silicon strip detectors (SSD) will be used in the two outer layers of the Inner Tracking System (ITS) of the ALICE experiment [1]. Two kinds of detectors may be considered: single-sided (SS) and double-sided (DS). Both types of detectors have been tested at IReS Strasbourg in the framework of R&D activities. Fairly extended tests of SS have already been presented in [2]. For these detectors a spatial resolution of about 7μm was found.

Using DS instead of two glued SS presents several advantages. It is possible to reduce the radiation length and also to match the charge signals collected on both sides, thus reducing the ambiguities due to multiple hits [3, 4].

Investigation of DS started at IReS with quality tests [5].

In this note, we present results of tests of a DS, obtained form CERN, performed with a 3 GeV pion beam from the Proton Synchrotron (CERN). A description of the experimental setup as well as of the characteristics of tested and reference detectors is given in section 2. In section 3, the charge matching between signals from both sides of the tested detector, produced by the same traversing particle, is studied. The influence of the incidence angle of particles on the spatial resolution of the tested detector is analysed. Finally, the contribution of multiple scattering to the impact point uncertainty is calculated and the corrected spatial resolution is extracted.

2 Experimental setup

2.1 Overview

The telescope used is sketched in Fig.1. It consists of four pairs of SS reference detectors with the tested DS in between. For each reference pair, one detector is measuring the horizontal coordinate (X), while the other gives the vertical one (Y). The tested detector may be rotated up to 45^o around the Y axis, parallel to the strip direction of the p-side.

A 7×7 mm^2 scintillator counter (not shown in the figure) located downstream delivers a trigger signal.

All detectors are AC coupled to low noise Viking readout electronics [6], connected directly to Sirocco ADC's [7]. Data control and acquisition are performed by VME electronic modules. The on-line program is based on Microdas software, using the OS9 operating system, implemented by the LEPSI group at Strasbourg. The operating conditions are described in these latter references.

2.2 Characteristics of the reference detectors

The reference detectors are all 14×14 mm^2 with 50 μm pitch and 300 μm thick. The detectors have 256 readout strips each. They have also intermediate strips, not connected to the readout electronics, but collecting charges by capacitive coupling.

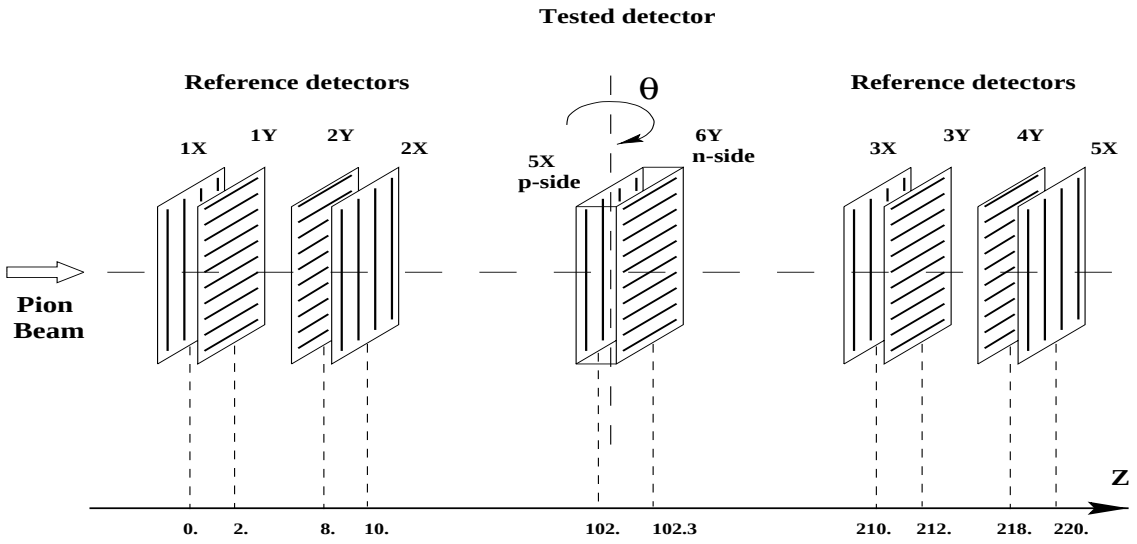

Figure 1: The detector telescope used in the pion beam tests. The relative positions of all detectors are reported (in mm) with respect to the first reference detector - 1X. The detectors are identifed as iX and iY according to the direction for which the spatial resolution is measured.

2.3 Characteristics of the tested detector

The tested DS is 20×20 mm^2 in size, the pitch is 50 μm and the thickness 300 μm. There are no intermediate strips between the readout strips. The stereo angle between the strips is of 90^o. Each side have 384 strips and is connected to three Viking chips. The applied depletion voltage is 80 V.

3 Pion beam tests

The data analysis is based on a computer program initially developped by R.Turchetta [8]. The full procedure for extracting the physic signal from raw data by selecting the cluster of strips, activated by a particle going across the detector, is described in [2].

3.1 Charge matching

Since DS has the advantage to allow charge matching, we have first examined this aspect. Fig.2 shows the distribution of the cluster pulseheights, readout from the p-side, versus the cluster pulseheights of the n-side, produced by the same traversing

particles. A good matching is obtained. This distribution may be fitted, with a linear function over the 200 - 1200 ADC count range, as:

$$H_{p-side} = -26.4 + 1.19\, H_{n-side} \ ,$$

where H_{p-side} and H_{n-side} are the cluster pulseheights from p-side and n-side, respectively. The constant term corresponds to systematic errors when determining cluster pulseheight values and, in an ideal case, should be equal to 0.

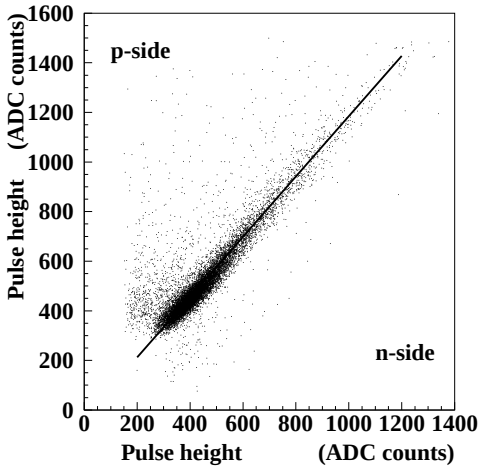

Figure 2: Distribution of the cluster pulseheights measured on the p-side versus the ones on the n-side for the same traversing particles. The solid line is a fit to the data (see text).

The second coefficient shows the correspondence between the pulseheights from both sides. This coefficient also depends on the gain of the electronics chains. Electronics are different, because one side is at ground potential and the other is floating. Furthermore, the measured noise on the p-side is half the one on the n-side, as illustrated in Fig.3. A rough estimate of the noise in equivalent electrons can be made knowing that the most probable charge deposition for a minimum-ionizing particle in 300 μm silicon is 25000 e^-. Indeed, according to Fig.6 (see later in 3.3.2), the most probable pulseheight is 414 ADC count. Hence 1 ADC count is equivalent to 60 e^-. Fig.3 shows a noise mean value of 4 ADC counts and 8 ADC counts for p-side and n-side, respectively, leading to 240 e^- for p-side and 480 e^- for n-side.

The distribution of deviations of the pulseheight values obtained from the fit is shown in Fig.4. A resolution of charge matching below 5% is calculated which is a satisfactory figure. The unfitted part of the distribution represents 8% of the total yield. It corresponds mostly to not-properly matched low p and n pulseheights. The reason maybe from various origins not firmly established at the moment.

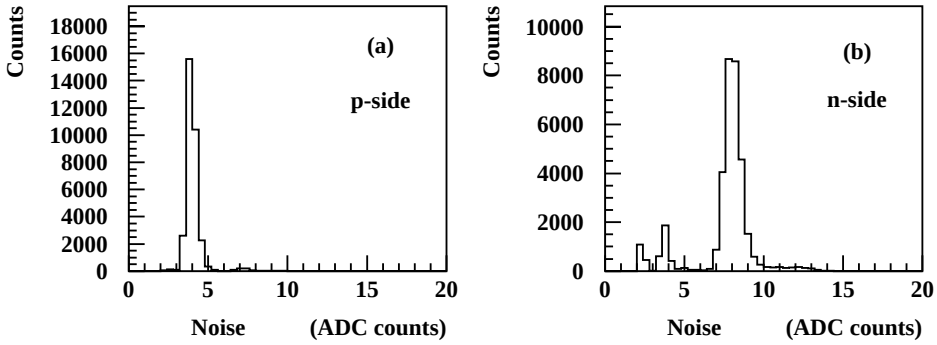

Figure 3: Noise distributions for clusters of (a) p-side and (b) n-side of the tested double-side silicon strip detector.

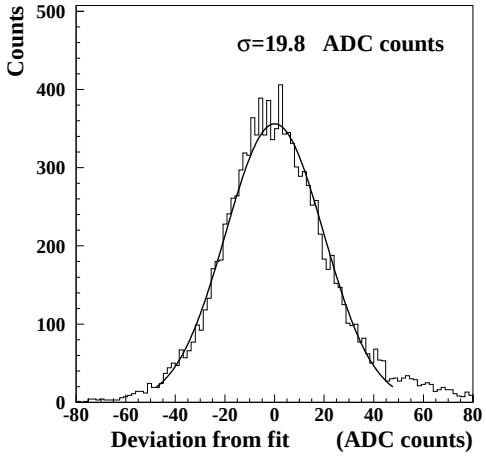

Figure 4: Distribution of deviations of the pulseheight values from the line (see Fig.2). Fitting this distribution with a Gaussian function yields the reported σ.

3.2 Spatial resolution of the reference detectors

Table 1 presents the spatial resolution σ for all SS reference detectors. It is obtained by fitting a Gaussian to the measured residual distribution (difference

between calculated particle track and measured track) as described in [2]. A typical residual distribution of a reference detector is shown in Fig.5.

Table 1: Spatial resolution for all SS reference detectors. The detectors are labeled as in Fig.1.

detectors	1X	2X	3X	4X
σ (μm)	3.7	3.8	3.8	3.7
detectors	1Y	2Y	3Y	4Y
σ (μm)	3.6	3.6	3.2	3.1

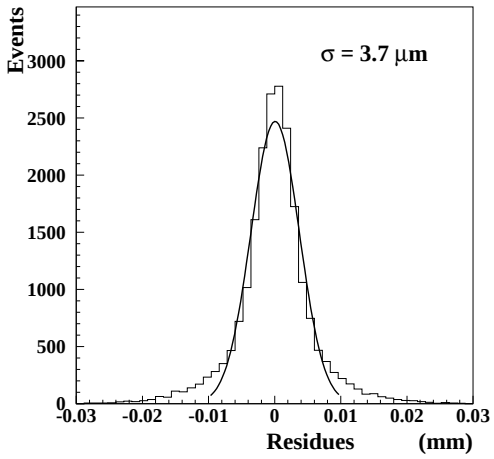

Figure 5: Residual distribution of the reference detector 4X. Fitting this distribution with a Gaussian function gives the indicated residual width.

These spatial resolution values may look fairly low. For this kind of Silicon detector, the spatial resolution is currently better than 1.5 μm. With a 3 GeV pion beam, we have a contribution from the multiple scattering to the measured position which deteriorates the spatial resolution.

3.3 Spatial resolution of double-sided detector – Influence of the particle incident-angle

In this section, results of tests of a DS for different particle incident-angles are presented. We will discuss first different algorithms for cluster finding. Then, the cluster pulseheight and the number of strips per cluster will be analysed for different track orientations. The spatial resolution on both sides of the tested detector will be extracted.

3.3.1 Cluster-finding algorithms

The rotation axis is parallel to the strip direction of the p-side of the DS, thus perpendicular to the strip direction of the n-side. The rotation angle is denoted θ and the incident angle is $90^o - \theta$. Since strips have different orientation on both side, the variation of θ leads to different effect.

Let us consider first the p-side. For tracks with normal incidence or slightly inclined, most of the charge is collected essentially by two strips. In this case, we used the η algorithm to determine the mean cluster position, as it is presented in [2]. But for larger incident angles, the charge is collected on more strips, increasing the cluster size. So, we have to change the cluster-finding algorithm for determining the mean position of the track, which is capital for the determination of the spatial resolution. The best algorithms for different incident angles are described in [9]. Thus , we used the η algorithm for $\theta = 0^o$ and $\theta = 15^o$, center-of-gravity (COG) for $\theta = 30^o$ and analog head-tail (AHT) for $\theta = 45^o$.

The mean position of the cluster for COG algorithm is given by

$$X_{COG} = \sum_{cluster} S_i x_i \Big/ \sum_{cluster} S_i \ ,$$

where x_i is the position of ith strip included in the cluster and S_i the signal readout on that strip. The sums are over all strips of the cluster.

For AHT algorithm, the equation giving the mean cluster position gets more complicated. Since the energy loss is proportional to the particle-path length in the silicon, the position can be defined in the following way:

$$X_{AHT} = \frac{x_h + x_t}{2} + \frac{S_h - S_t}{2S_\theta} P \ ,$$

where x_h and x_t are the position of the head and the tail of the cluster distribution, respectively; S_h and S_t are the readout signals on these strips. P is the readout pitch and S_θ is given by

$$S_\theta = \frac{S_0 P}{t \ \sin(\theta)} \ ,$$

where S_0 is the most probable signal released by a particle when $\theta = 0^o$ and t is the detector thickness.

Variations of θ have less important effect on the spatial resolution on the n-side of the detector. With increasing θ, the particle path lengthens and, as a consequence, the scattering of the charge cloud increases, but the whole charge remains mostly collected by nearly two strips. Thus, it remains possible to use η algorithm over a wide angle domain.

3.3.2 Cluster parameters of the tested detector

One of the sensitive parameter, directly correlated to the particle incident angle, is the cluster size. As was mentioned above, variation of θ should lead to larger change for the p-side than for the n-side. It can be accessed by comparing the mean number of strips per cluster for different angles. Table 2 presents the resulting mean number of strips per cluster for each side of the tested DS at $\theta = 0^o, 15^o, 30^o, 45^o$. While, the number of strips per cluster is hardly changing for the n-side, it increases drastically for the p-side when θ gets larger.

Table 2: Number of strips per cluster for different values of the rotation angle θ. Results for p-side and n-side of tested double-sided silicon strip detector are presented.

θ	**p-side** number of strips per cluster	**n-side** number of strips per cluster
0^o	1.64	2.24
15^o	2.50	2.25
30^o	4.22	2.32
45^o	6.40	2.40

The cluster pulseheight is another parameter, dependent on the incident angle. The minimum ionizing particle traversing the silicon detector looses energy in proportion of its path length inside the detector. The deposited energy yields electron-hole pairs. The holes are collected on the p-side and the electrons on the n-side, respectively. Thus, the cluster pulseheight changes with θ for both sides.

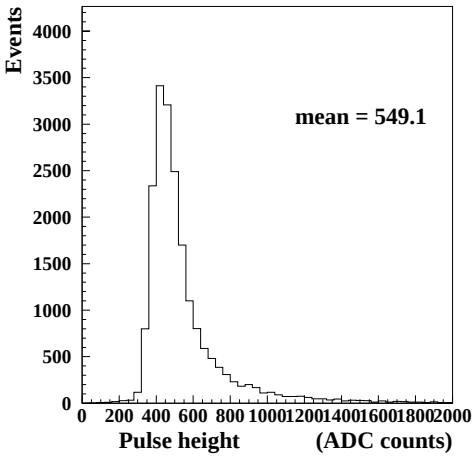

Figure 6: Cluster pulseheight of p-side of the tested DS silicon strip detector for tracks with normal incidence.

The distribution of the cluster pulseheight for $\theta = 0^o$ for the tested DS is given in Fig.6. It is typical of a Landau pattern. For comparing cluster pulseheight at different incident angles, we used the mean values of the distributions. Table 3 shows the mean values of cluster pulseheight for different rotation angles. The increase on both side is directly correlated with the track length in the silicon which increases as $1/cos\theta$. This correlation is nicely displayed on Fig.7.

Table 3: Cluster pulseheight of the tested DS for different rotation angles.

θ	**p-side** Cluster P-H (ADC counts)	**n-side** Cluster P-H (ADC counts)
0^o	549.1	475.2
15^o	567.0	486.0
30^o	640.3	531.1
45^o	762.4	621.1

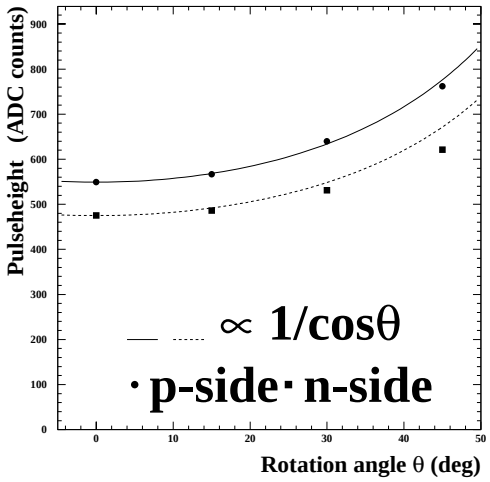

Figure 7: Correlation between the mean cluster pulseheight (points and squares) and the track length in the silicon which is proportional to $1/cos\theta$.

3.3.3 Spatial resolution of the tested detector

As an example, Fig.8 presents two residual distributions with reported spatial resolution for the p-side of the tested DS for normal and 45^o inclined tracks. All residual widths for both sides of the tested detector and for different rotation angles are given in Table 4.

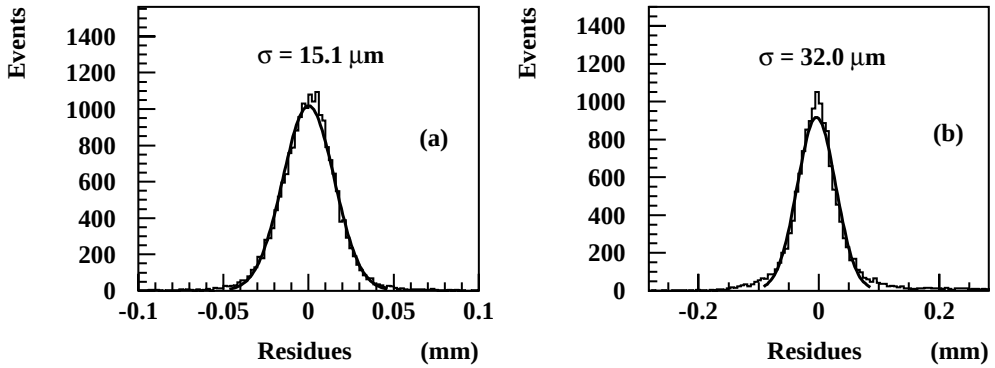

Figure 8: Residual distributions of p-side of the tested DS silicon strip detector for (a) normal (0^o) and (b) 45^o inclined tracks. Fitting these distributions with a Gaussian function (solid curves) gives the indicated residual widths.

Table 4: Spatial resolution of the tested DS. The residual widths for both sides and for different rotation angles are reported.

θ	**p-side** σ (μm)	**n-side** σ (μm)
0^o	15.1	18.1
15^o	15.8	18.1
30^o	19.3	18.5
45^o	32.0	21.1

Between $\theta = 0^o$ and 45^o, the spatial resolution increases from 15 μm to 32 μm, these figures are acceptable.

4 Simulation of multiple scattering

The multiple scattering of a 3 GeV pion beam gives substantial contribution to the impact point error, thereby, worsening the spatial resolution. To estimate this contribution to the spatial resolution of the tested DS detector, we have run some simulation. It incorporates the geometry of the setup used with the 3 GeV pion beam. All materials on the beam path (air, mylar, aluminium) have been taken into account.

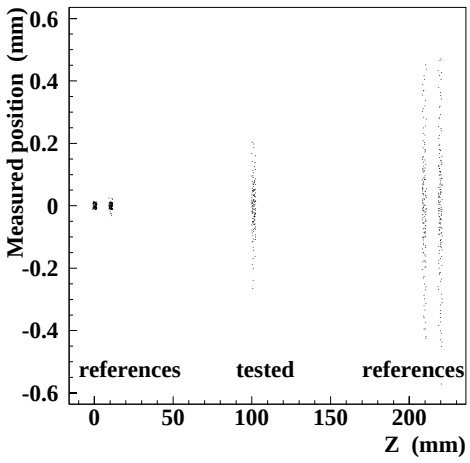

Figure 9: Simulated distribution of a 3 GeV pion beam divergence in the used test setup.

The program calculates the divergence of the pion beam from normal incidence, due to Coulomb scattering in all media of the experimental setup and gives the contribution from multiple scattering.

Initial resolutions for tested and reference detectors have been assumed as:

$$\sigma_{test} = 5\mu\text{m} \ , \ \sigma_{\text{ref}} = 1\mu\text{m}.$$

The resolution of tested detector was calculated in three different cases. First, when the simulation of multiple scattering is turned on and the detectors have the initial resolutions σ_{test} and σ_{ref}. The divergence of the pion beam in this case is shown in Fig.9, and a resolution of:

$$\sigma_{test_1} = 12.31 \ \pm \ 0.09 \, \mu\text{m}$$

is found for the tested DS.
Second, when the simulation of the scattering is turned off and the initial resolutions remain σ_{test} and σ_{ref}, then:

$$\sigma_{test_2} = 4.98 \ \pm \ 0.04 \, \mu\text{m} \, .$$

The contribution of multiple scattering can then be obtained from:

$$\sigma_{SCATT} = \sqrt{\sigma^2_{test_1} - \sigma^2_{test_2}} = 11.26 \ \pm \ 0.1 \, \mu\text{m} \, .$$

The third case is like a check-test; the simulation of the scattering is turned on but the detectors are taken as ideal detectors (σ_{test} and σ_{ref} are not taken into account). Then, the obtained resolution should be equal to the contribution of multiple scattering only. There, one finds:

$$\sigma_{test_3} = 11.25 \ \pm \ 0.08 \, \mu\text{m} \, .$$

As expected, $\sigma_{SCATT} \approx \sigma_{test_3}$. The same simulation has been runned with different inputs for σ_{test} and σ_{ref}, no appreciable dependence on σ_{SCATT} has been found.

By taking into account σ_{SCATT}, obtained from the simulation, it is possible to correct the measured resolution σ_p(MEAS) and σ_n(MEAS) for both sides of the tested DS detector for normal incidence, as:

$$\sigma_{p-side} = \sqrt{\sigma_p(\text{MEAS})^2 - \sigma^2_{\text{SCATT}}} = 10.1 \, \mu\text{m}$$

$$\sigma_{n-side} = \sqrt{\sigma_n(\text{MEAS})^2 - \sigma^2_{\text{SCATT}}} = 14.2 \, \mu\text{m} \ ,$$

where

$$\sigma_p(\text{MEAS}) = 15.1 \, \mu\text{m} \quad \text{and} \quad \sigma_{\text{n}}(\text{MEAS}) = 18.1 \, \mu\text{m} \quad \text{as takenfrom Table 4.}$$

This yields satisfactory spatial resolution on both sides.

5 Conclusion

In this note, we have presented results from tests, with a 3 GeV pion beam, of a double-sided silicon strip detector with a stereo angle of 90^o. A good matching of the charges collected on both sides is achieved with better than 5% resolution.

The algorithms η, center-of-gravity and analog head-tail have been used to extract the spatial resolution at different beam incident-angles. The spatial resolution for both sides is close to 15 μm at normal incident beam. It increases up to 32 μm at 45^o.

Investigation of multiple scattering has been done. Its contribution to the spatial resolution was calculated. Then, the corrected spatial resolution of the detector for normal incidence was found equal to 10 μm and 14 μm for p-side and n-side, respectively.

References

[1] ALICE Technical Proposal, CERN/LHCC 95-71, LHCC/P3, December 1995

[2] L.Arnold, J.P.Coffin, P.Fintz, G.Guillaume, F.Jundt, C.Kuhn, J.R.Lutz, P.Pagès, S.Pozdniakov, F.Rami, K.Šparavec, L.Tizniti, C.Colledani, W.Dulinski, R.Turchetta, C.Roy, *Experimental study of the spatial resolution of silicon microstrip detectors for the Inner Tracking System of the ALICE Detector.* ALICE/97-12, Internal Note/ITS April 97

[3] M.Monteno, ALICE Note/SIL/94-13

[4] T.Ohsugi, Y.Unno and N.Tamura, *Development and application of semiconductor tracking detectors.* Nucl. Inst. and Meth. in Phys. Res. **A383** (1996) 349-361

[5] L.Arnold, T.Cambon, J.P.Coffin, P.Fintz, G.Guillaume, F.Jundt, C.Kuhn, J.R.Lutz, P.Pagès, S.Pozdniakov, F.Rami, K.Šparavec, W. Dulinski, *Quality tests of double-sided silicon strip detectors.* Internal ALICE Note/SIL/97-30

[6] S.Masciocchi, E.Nygård, A.Rudge, O.Toker, P.Weilhammer, *VIKING, a CMOS low noise monolithic 128 channel frontend for Si-strip detector readout.* Nucl. Inst. and Meth. in Phys. Res. **A340** (1994) 572-579

[7] N.Bingefors, M.Burns, *SIROCCO IV : front end readout processor for DELPHI microvertex.* CERN/PPE 88-088

[8] R. Turchetta, *Thèse de l'Université Louis Pasteur, Strasbourg.* CRN/HE 91-07

[9] R. Turchetta, *Spatial resolution of silicon microstrip detectors.* Nucl. Inst. and Meth. in Phys. Res. **A335** (1993) 44-58